Inclusion Investigation during Clean Steel Production at Baosteel

Lifeng Zhang, Brian G. Thomas
Dept. of Mech. and Industrial Engr., Univ. of Illinois
Urbana, IL61801, U.S.A.
Tel: 1-217-244-4656, Fax: 1-217-244-6534
zhang25@uiuc.edu, bgthomas@uiuc.edu

Kaike Cai
School of Metallurgy, Univ. of Sci. & Tech. Beijing
Beijng 100083, P.R.China

Jian Cui, Lixin Zhu
The Technical Research Center, Baosteel CO., Baoshan
Shanghai 201900, P.R.China

Key words: Steel cleanliness, Inclusions, Ladle, Tundish, Mold, Mathematical simulation, Fluid flow

INTRODUCTION

The importance of clean steel to product quality is increasingly being recognized. Controlling the size distribution, morphology, and composition of the non-metallic oxide inclusions is the first demand for clean steel. In addition, sulfur, phosphorus, hydrogen, nitrogen and even carbon [1, 2] also should be controlled, because these elements affect steel mechanical properties. For example, formability, ductility and fatigue strength worsen with increasing sulfide and oxide inclusion content. Lowering C and N enhances strain aging and increases ductility and toughness. Solid solubility, hardenability and resistance to temper embrittlement can be enhanced by lowering P. [1] The definition of 'clean steel' varies with steel grade and its end use. For example, IF steel requires C and N both <30ppm; line pipe requires S, N and O all <30ppm; HIC resistant steel requires P≤50ppm and S≤10ppm, and bearing steel requires the total oxygen less than 10ppm.[3] In addition, many applications restrict the maximum size of inclusions [3, 4], so the size distribution of inclusions is also important. The control of steel cleanliness has been extensively reviewed by Kiessling in 1980 [5], McPherson and McLean in 1992 [6], Mu and Holappa in 1993 [7], Cramb in 1999 [4], and Zhang and Thomas in 2003 [3]. The current paper reports on steel cleanliness investigations and mathematical simulations of fluid flow and inclusion behavior in ladle, tundish and continuous caster to improve understanding of clean steel production.

INDUSTRIAL EXPERIMENTS

Experimental Methods

Baosteel, P.R.China, produces over 11.5 million tonnes steel in 2001 including 880,000 tonnes IF steel. At the #1 steel plant of Baosteel, there are three 300-tonne BOF steelmaking furnaces, one CAS-OB, two RH degassers, refining apparatus, one IF furnace and two continuous slab casters. During the past ten years, steel

cleanliness has been investigated for **L**ow **C**arbon **A**l-**K**illed Steel (**LCAK** Steel) (1992, 1994), desulfurized and dephosphorized LCAK steel (1995) and Ultra-LCAK steel (1996). The experimental heat conditions are listed in **Table I**. The ladle capacity is 300 tonne, with 3.2m bottom diameter, 3.8m top diameter and 4.5m height. The argon flow rate is 0.5 Nm^3/min for the CAS treatment. Several flow control configurations are used in the 60 tonne two-strand tundish, included in Table I. **Figure 1** shows that the standard tundish B has one weir and one dam on each side (1^{st} - 4^{th} heats) and tundish C has one weir containing a CaO filter and two dams on each side (5^{th}-7^{th} heats). Tundish D is the same as tundish C with the weirs extended to the bottom. The slab section is 1300mm×250mm and the casting speed is 1.2m/min. The mold is 900m in length. The SEN has 140mm inner bore, 15^o down, 65mm×80mm section outports and 300mm submergence depth. The argon gas injection at the SEN is 5-10 Nl/min at the upper slide gate and 10Nl/min at the upper nozzle.

Table I Operational conditions for different heats

Heats	Ladle refining	Tundish (each side)	Mold	Year
1^{st} heat	CAS-OB	1 weir, 1 dam; without shrouding from ladle to tundish (Tundish B)		1992
2^{nd} heat	CAS-OB	1 weir, 1 dam (Tundish B)		1992
3^{rd} and 4^{th} heats	RH	1 weir with CaO filter, 1 dam	3^{rd} strand	1994
		1 weir, 1 dam (Tundish B)	4^{th} strand	
5^{th}, 6^{th}, and 7^{th} heats	RH	1 weir with filter, two dams (weir doesn't touch bottom) (Tundish C)		1995
8^{th} and 9^{th} heats	RH	1 weir with filter, two dams (weir touches bottom) (Tundish D)		1996

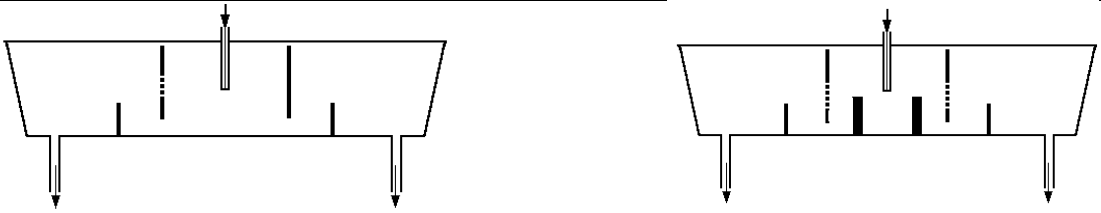

Fig. 1 Schematic of tundish B (left) and C (right)

The sampling includes several slag and molten steel samples taken before, during and after steel refining, at tundish and mold, and steel samples at different places in the slab. Ladle steel samples were taken 500-600mm below the top slag in the ladle, tundish steel samples from 300mm above its outlet, and mold steel samples from 150mm below the meniscus and 300mm away from the SEN outport. The analysis includes chemical composition of the slag and steel samples, microscope observation for microinclusions, slime extraction for macroinclusions, SEM analysis for the morphology and composition of inclusions. In the text, "macroinclusions" is used to express the mass of large inclusions (>50μm in diameter) extracted per unit mass of steel sample dissolved by Slimes test; "microinclusions" represents the inclusion content in number per unit area observed by microscope. The removal fraction of total oxygen (or inclusions) from vessel i to vessel j is defined by:

$$f_{ij} = \frac{T.O._i - T.O._j}{T.O._i} \times 100\% \qquad (1)$$

where $T.O._i$ is the cleanliness value in vessel i (ladle before steel refining, ladle after steel refining, tundish or mold), $T.O._j$ is the cleanliness value in vessel j (ladle after steel refining, tundish, mold, or slab).

Control of Total Oxygen, Nitrogen, Sulfur, Phosphorus, and Carbon in Steel

Total oxygen- Many techniques are used to lower the total oxygen in steel, such as controlling slag carryover during BOF tapping by a slag ball in order to lower the reoxidation by FeO and MnO, increasing argon flow

rate and treatment time during RH treatment, employing flow control devices in the tundish to increase the residence time of the molten steel and thus improve inclusion removal, using basic lining refractory (MgO based) in the tundish to absorb inclusions and prevent reoxidation from SiO_2, replacing rice hulls with a new tundish flux, and high CaO content in the mold flux to absorb floated inclusions. The measured total oxygen distribution along the slab thickness is shown in **Fig.2**. The total oxygen in slab is 10-32ppm, averaging 24 ppm. Slight peaks are sometimes found at the centerline and occasionally at the inner radius half thickness of the slab.

Nitrogen- Nitrogen during BOF steelmaking fluctuates from 11 to 43ppm. Normally, a large nitrogen content at tapping tends to a large nitrogen content in the slab. Thus the control of nitrogen should mainly focus on lowering the nitrogen content during BOF blowing and preventing nitrogen pickup during tapping, steel refining, and continuous casting. The industrial experiments indicate that when [N] is less than 25ppm before RH treatment, [N] can not be further lowered by RH treatment. The current nitrogen pickup from ladle to slab is 3-7ppm. The shrouding system is critical to prevent air absorption. As evidence, accidentally pouring from ladle to tundish without shrouding (1^{st} heat) induced 24.4ppm nitrogen pickup, and this value lowered to 3.7ppm with shrouding (2^{nd} heat).

Sulfur- The initial sulfur content of the molten iron is around 200ppm. After molten iron desulfurization by injecting CaC_2 powder, sulfur decreases to around 10ppm. It is important to remove the top slag quickly after desulfurization in order to decrease sulfur pickup. During BOF steelmaking process, there is 10-30ppm sulfur pickup, mainly from the lime and scrap. There is also 1-6ppm sulfur pickup during RH treatment from alloys added, slag, and steel remaining in the RH before treatment. During continuous casting of heats 5-7, [S] decreases by 2-4ppm, possibly because the MgO-CaO lining refractory of the tundish can remove some sulfur by the following reaction

$$(CaO)+2/3[Al]+[S]=(CaS)+1/3[Al_2O_3]. \quad (2)$$

Thus the main way to control sulfur is to lower the sulfur pick-up during BOF steelmaking and secondary refining. The best practice produced slabs averaging 21ppm [S] (Fig.2).

Phosphorus- Double BOF blowing was used to decrease phosphorus (5^{th} -9^{th} heats). Holding the melt temperature at 1340-1350 ^oC and slag basicity >3.0 in BOF favors dephosphorization. Phosphorus pickup occurs because the tundish flux contains 0.016% P. Heat 6 has 10ppm [P] pickup during tapping. The best practice produced slabs averaging 20ppm [P], with slightly higher [P] concentrated near the slab centerline. (Fig.2).

Carbon -[C] after RH treatment is around 20ppm, and 8-10ppm [C] pickup occurs during continuous casting, thus slabs have about 30ppm [C]. Mathematical simulations suggest that at RH, by enlarging the snorkel diameter to 750mm, increasing argon flow rate to 3.0 Nm^3/min, blowing 16Nm^3/min oxygen at 0-5min, and quickly decreasing the vacuum chamber pressure, [C] can be lowered from 400ppm to 21ppm after 10min, and to 13ppm after 20min. [8] [C] within the inner radius side of the slab is higher than elsewhere (Fig.2).

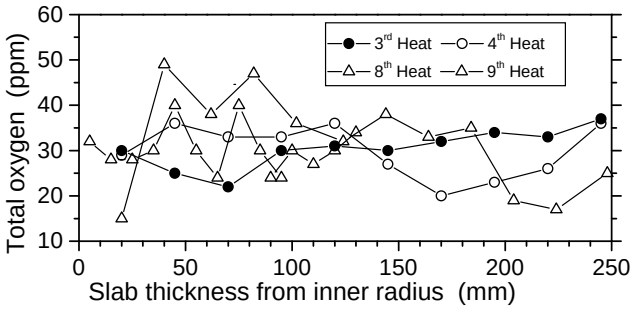

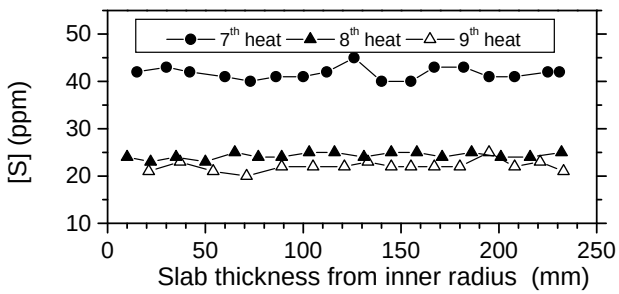

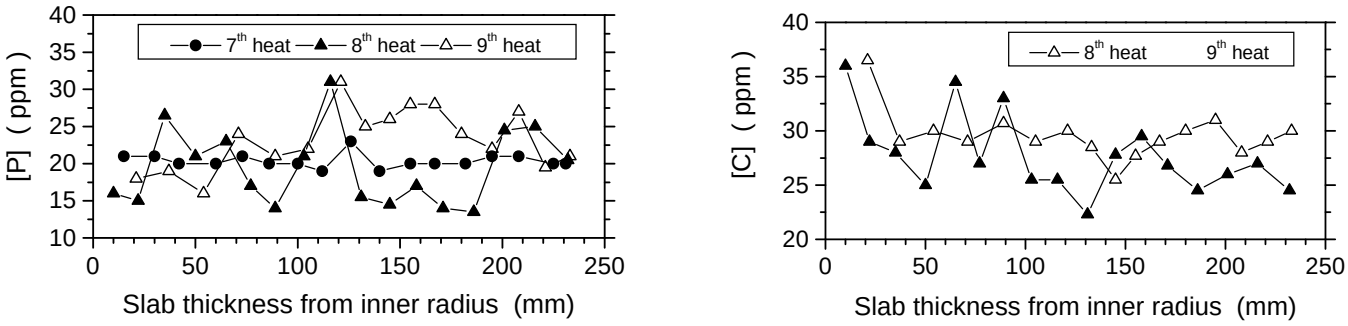

Fig.2 The distribution of the total oxygen, sulfur, phosphorus, and carbon along the slab thickness

Total content of these elements in the slab- Table II shows the total oxygen, nitrogen, phosphorus, sulfur, and carbon in the slab. In this table, "Mean" is the averaging value along the slab thickness, and "Min" is the minimum value along the slab thickness. Currently the best practice produces T.O.+[N]+[P]+[S] around 80ppm, and [C]+T.O.+[N]+[P]+[S] around 100ppm in the slab.

Table II Mean and minimum values in ppm of T.O., [C], [P], [S], [C] in the slab

	T.O.		[N]		[P]		[S]		[C]		In total	
	Mean	Min	Mean	Min	Mean	Min	Mean	Min	Mean	Min	Mean	Min
5th heat	17	14	15	13	20	17	31	26			83	70
6th heat	18	14	37	34	30	17	36	34			120	99
7th heat	14	11	26	22	20	19	42	40			102	92
8th heat	32	15	31	24	19	13	24	22	28	13	135	87
9th heat	30	24	27	23	23	14	21	20	30	14	130	95

Inclusion Removal at Every Step

Argon bubbling (CAS-OB)- For heats 1 and 2, the steel refining was carried out by CAS-OB. The T.O. is lowered from 208ppm to 173ppm, and macroinclusions decrease from 205 to 178 mg/10kg steel.

RH treatment- Figure 3 shows the fraction of the total oxygen (f_{ij}) removed from the ladle by comparing samples taken within ~1min after aluminum addition (i) and at the end of RH treatment (j). The result for different RH deoxidation times suggests an optimum treatment time of 12-15min. Beyond this optimum time, the oxygen removal efficiency may decrease due to lining refractory erosion. Also, excessive stirring is detrimental because it may expose an "eye" or slag-free region of the steel surface to air reoxidation and perhaps even slag entrainment. **Figure 4** shows that RH treatment can remove up to 90% of macroinclusions, 50-70% of microinclusions, and 70-90% of the T.O.. Alumina in the ladle slag during RH treatment increases 8-13%.

Oxygen balance in the ladle during RH treatment and in the tundish – Reoxidation to form alumina in the ladle during RH treatment is mainly caused by SiO_2 in slag and lining refractory, MnO and FeO in ladle slag by the following reaction.

$$3/2(SiO_2)+2[Al]=(Al_2O_3)+3/2[Si] \quad (3)$$
$$3(MnO)+2[Al]s = (Al_2O_3)+3[Mn] \quad (4)$$
$$3(FeO)+2[Al]s = (Al_2O_3)+3[Fe] \quad (5)$$

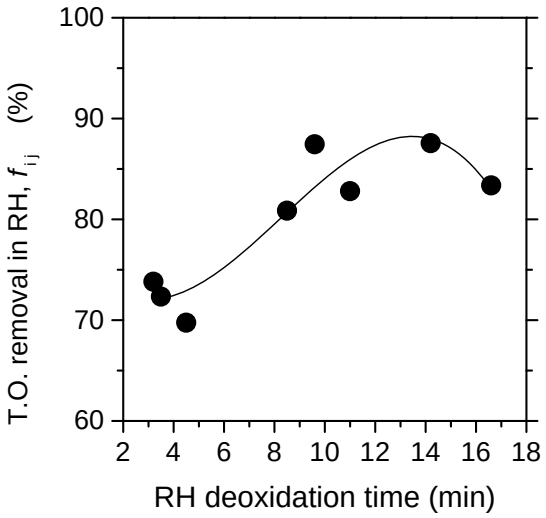

Fig.3 T.O. removed during RH treatment

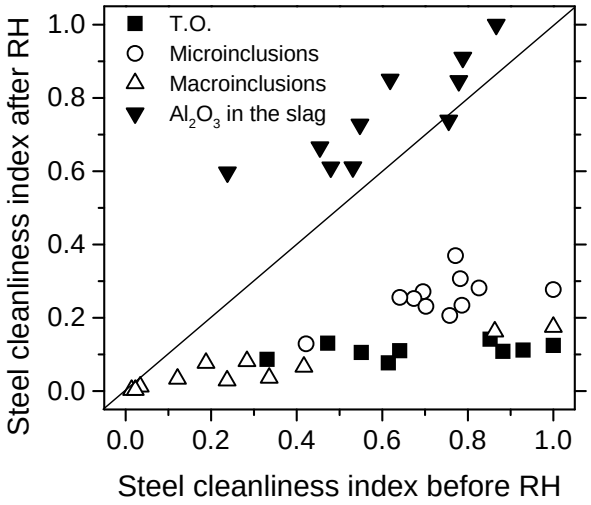

Fig.4 Steel cleanliness before and after RH

MnO and FeO content in the ladle slag is around 16-17%. Larger FeO+MnO content in the ladle slag corresponds to a higher total oxygen (**Fig.5**). Controlling the slag carryover from the steelmaking furnace during tapping and ladle slag reduction treatment are used to lower FeO and MnO in the ladle slag [3]. The measured difference of [Mn], [Si] before and after RH treatment (Δ[Mn], Δ[Si]) can be converted to absorbed oxygen (Δ[O]) and reoxidized aluminum (Δ[Al]) by the basic chemical balance of reactions (3)-(5), as given in **Table III**. Reoxidation of [Al] by FeO in the slag can be estimated by $\Delta[Al]_{FeO}=[(\%FeO)/(\%MnO)] \times \Delta[Al]_{MnO}$, where (%FeO), and (%MnO) are FeO and MnO content in the ladle slag, and the oxygen absorbed to steel by the reoxidation from FeO can be obtained by $\Delta[Al]_{FeO}$. The total oxygen from reoxidation, ΣΔ[O], is the sum of these 3 sources, adjusted again for stoichiometry. Using the same method as for the ladle, reoxidation in the tundish is given in **Fig. 6**, which suggests that the main reoxidation is from FeO and MnO in the ladle slag, reoxidation from SiO_2 is also serious when the tundish flux has 18% SiO_2, and around 2-10 ppm reoxidation is from air absorption. The total oxygen balance in the ladle during RH treatment and in the tundish during continuous casting is therefore given in **Table IV**. Reoxidation accounts for about 20% of the T,O, after RH and 50% of the T.O. in the tundish.

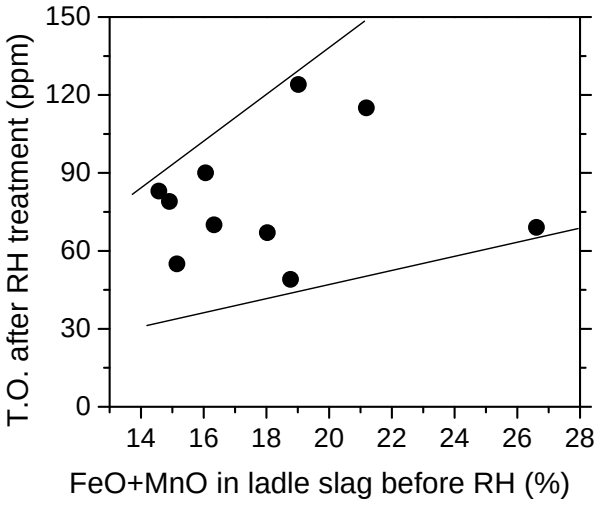

Fig. 5 The T.O. *versus* FeO+MnO in the ladle slag

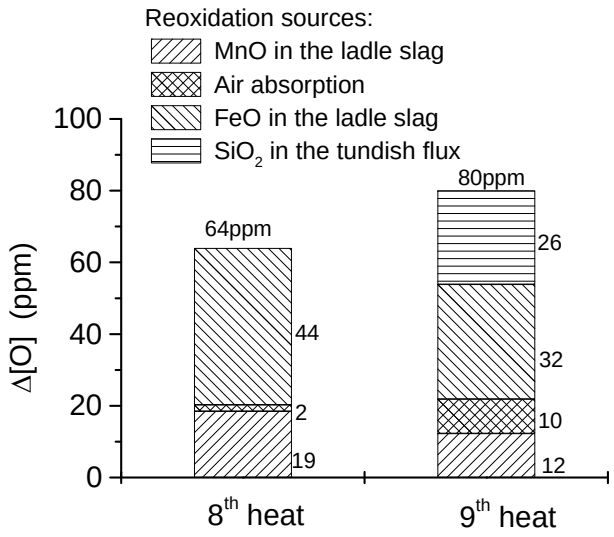

Fig.6 Quantitative reoxidation sources in CC tundish

Table III Steel reoxidation during RH treatment

	Δ[Si] (%)	Δ[Mn] (%)	$\Delta[Al]_{SiO2}$ (%)	$\Delta[Al]_{MnO}$ (%)	$\Delta[Al]_{FeO}$ (%)	ΣΔ[Al] (%)	$\Delta[O]_{SiO2}$ (ppm)	$\Delta[O]_{MnO}$ (ppm)	$\Delta[O]_{FeO}$ (ppm)	ΣΔ[O] (ppm)
8th heat	0.003	0.01	0.004	0.003	0.010	0.017	34	25	76	135
9th heat	0.003	0.01	0.004	0.003	0.012	0.019	34	25	90	149

Table IV Total oxygen balance in the ladle during RH treatment and in the tundish

	T.O. during RH Treatment (ppm)					T.O. in the Tundish (ppm)			
	Before RH	ΣΔ[O]	After RH	T.O. sources		ΣΔ[O]	Tundish	T.O. sources	
				Initial oxygen	Reoxidation			Ladle	Reoxidation
8th heat	541	135	90	72	18	64	60	35	28
9TH heat	635	149	79	64	15	80	49	25	25

Inclusion removal in tundish- Alumina in the tundish slag (initially 0.5%) increases to 16% at 49min for heat 8, and from 2% to 12.9% at 42min for heat 9. **Table V** shows the removal fraction of the T.O., microinclusions and macroinclusions from ladle after RH (i) to tundish (j), which suggests that more inclusions are removed in the tundish with each side having two dams and a weir containing filters (Tundish C, heat 6) than the tundish with only one dam, one weir and no filters on the measured side (Tundish B, heats 3 and 4, strand 4).

Table V Measured removal fractions of inclusions from ladle to tundish

		Tundish B		Tundish C		
		Heat 3	Heat 4	Heat 5	Heat 6	
T.O. (ppm)	Ladle	103	70	70	67	
	Tundish	81	63	57	44	
	f_{ij}	**21%**	**10%**	**19%**	**34%**	
Microinclusions (#/mm^2)	Ladle	7.2	8.4	8.1	10.8	10.8
	Tundish	5.1	6.0	7.2	5.1	3.2
	f_{ij}	**29%**	**28%**	**11%**	**53%**	**70%**
Macroinclusions (mg/10kg steel)	Ladle	66.0	138.9	16.8	94.3	
	Tundish	32.6	36.9	9.7	9.4	
	f_{ij}	**51%**	**74%**	**43%**	**90%**	

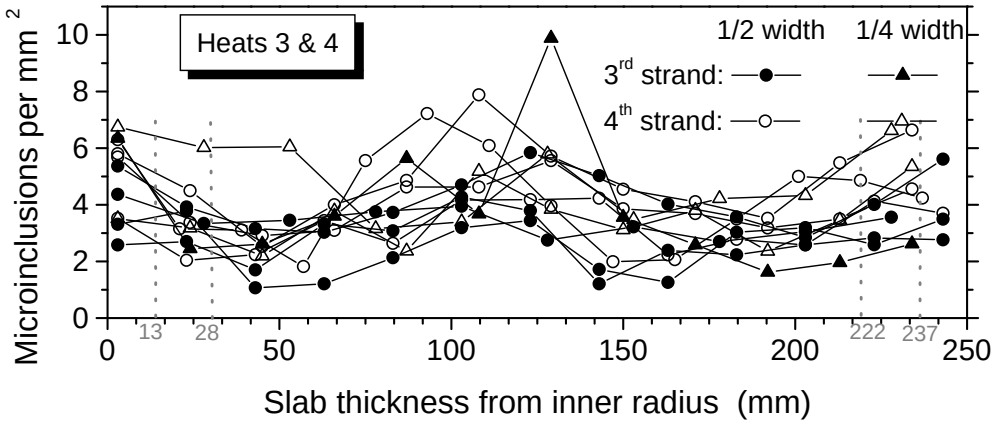

Fig. 7 Microinclusions distribution along the slab thickness with (strand 3) and without (strand 4) tundish filters

Steel cleanliness of slab- The distribution of inclusions along the slab thickness measured from microscope observations is shown in **Fig. 7**, which suggests that: 1). Inclusions concentrate more in the 20mm thickness nearest the slab surface; 2). Some slabs have occasional accumulation at the ½ and the ¼ slab thickness from the inner radius; 3). Filters in the tundish are effective at lowering microinclusion levels. Further investigation indicates that this inclusion accumulation is more prevalent in places such as the slab head and tail cast during unsteady conditions, as shown in **Fig.8**, from sulfur print detection. Microscope observation and SEM detection suggest that this inclusion accumulation mainly induced by the entrapment of dislodged clogged materials from the SEN during the ladle change. A typical inclusion in the slab head containing both clogged materials and some SEN surface refractory is analyzed in **Table VI**. Slag inclusions are mainly entrapped at the surface of the slab, as shown in **Fig.9**.

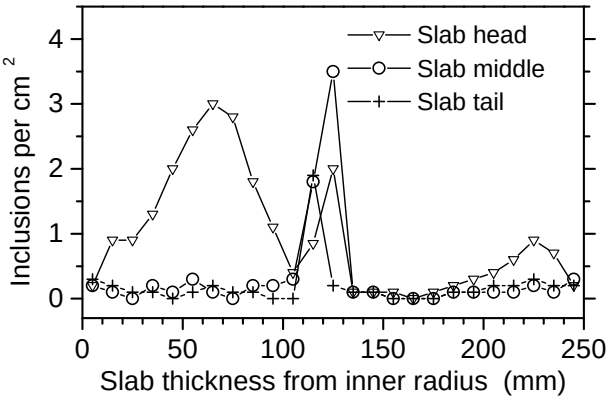

Fig. 8 Inclusion distribution along the slab thickness by sulfur print

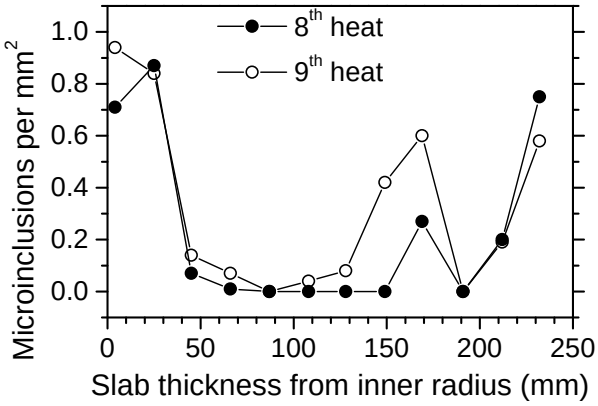

Fig.9 Slag inclusion distribution along the slab thickness

Table VI Comparison between slags, SEN clogging materials and the typical inclusion accumulated at the ¼ thickness of slab head

	Al_2O_3	SiO_2	FeO	Na_2O	Cr_2O_3	CaO	ZrO_2	S	F	C
Tundish powder	1.5	78.9	1.1							10.5
Mold flux	1.7	39.4		12.8		36.9			5.5	3.5
Initial layer of SEN	40.34	37.19	19.26	0.57	1.09	0.37	0.49	0.69		
Clogging materials 1	97.47	2.37	0	0.08	0	0	0	0		
Clogging materials 2	72.82	24.31	0.78	0.42	0.83	0.84	0	0		
Clogging materials 3	92.26	3.65	3.54	0.16	0	0.62	0	0.03		
Typical Inclusion	90.93	2.24	3.92	0	0	0.38	1.78	0.74		

Total oxygen evolution from ladle to slab- Based on averaging 9 heats, the T.O is 428ppm before steel refining, 101ppm after steel refining, 66ppm in the tundish, 48ppm in the mold, 29ppm in the slab (**Table VII**). Of the total oxygen in the ladle, the tundish removes 35%, 18% attach to the SEN walls, and the mold removes 19%. Of the total oxygen in the tundish, 27% attach to the SEN walls, and the mold removes 29%. Because tundish samples are taken 300mm above tundish outlet, and mold samples are taken 300mm away SEN outport and 150mm below meniscus, thus the removal fraction by the SEN may be exaggerated and contain contributions from both tundish and mold removal.

Table VII The total oxygen in the ladle, tundish, mold and slab (ppm)

	Ladle refining	Before refining	After refining	Tundish	Mold	Slab
1st Heat	CAS	330	230	107	108	49
2nd Heat	CAS	200	153	93	90	40
3rd Heat	RH	433	103	61	30	30
				81	45	30
4th Heat	RH	367	70	57	36	
				63	38	
5th Heat	RH	407	70	57	21	17
6th Heat	RH	350	67	44	22	18
7th Heat	RH	390	49	51	51	14
8th Heat	RH	747	90	60	46	32
9th Heat	RH	632	79	49	44	30
Average		428	101	66	48	29

Inclusion Morphology, Composition and Size Distribution Evolution

The morphology, composition and possible sources of typical inclusions found in steel samples from the ladle, tundish and mold are shown in **Figs 10** and **11**. The morphologies include: i) angular aluminate (Fig.10 d,f and Fig.11 c); ii) alumina cluster (Fig.10b,e); and iii) spherical silicate (Fig.10a,c and Fig.11a,b). The possible sources are deoxidation products, reoxidation product, slag entrapment or broken refractory lining bricks.

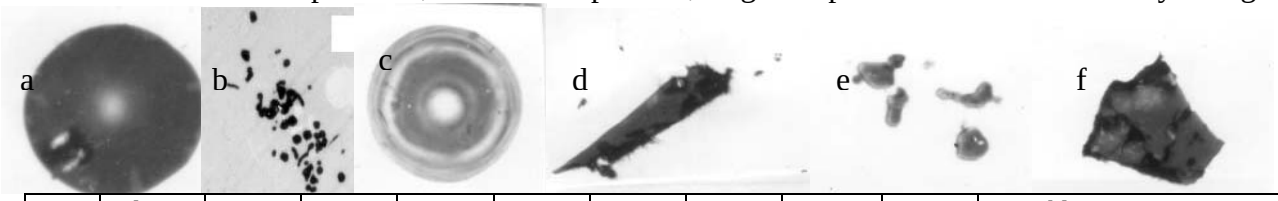

	Al_2O_3	SiO_2	CaO	MnO	FeO	MgO	K_2O	Na_2O	TiN	Possible source
a	1.2	56.4	0.5	5.8	20.3	10.1	0.3	5.1	0.3	Ladle slag
b	71.8	0.7	/	0.2	24.3	/	/	/	2.9	Deoxidation or reoxidation product
c	13.7	44.0	28.7	0.8	2.5	2.9	0.1	3.7	3.7	Mold flux
d	98.4	0.4	/	/	/	/	/	0.1	/	Deoxidation product
e	94.4	3.4	/	/	1.8	/	/	/	0.4	Deoxidation or reoxidation product
f	92.8	2.7	/	/	2.9	/	/	/	1.6	Refractory

Fig.10 Typical inclusions observed by microscope in the ladle (a) tundish (b), mold (c,d) and slab (e,f)

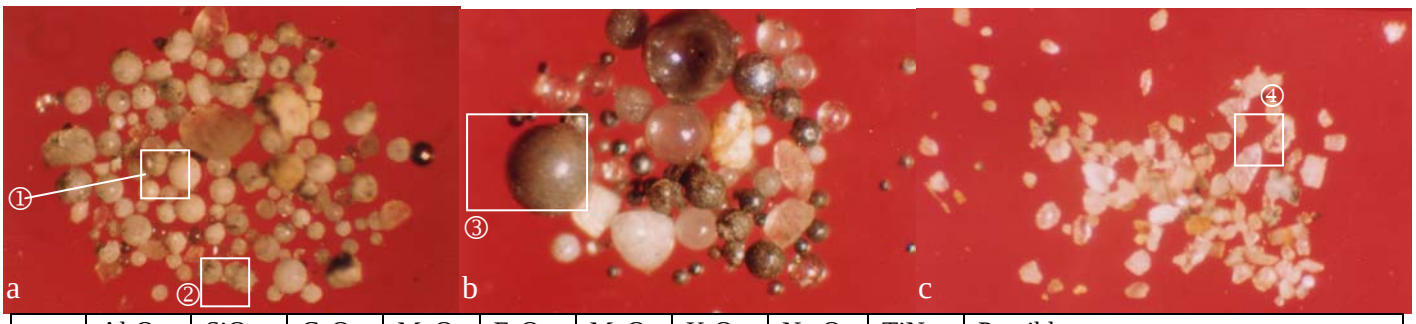

	Al_2O_3	SiO_2	CaO	MnO	FeO	MgO	K_2O	Na_2O	TiN	Possible source
①	/	79.1	/	20.0	0.7	0.1	/	/	0.1	Ladle slag
②	85.5	/	9.6	/	4.5	/	/	/	/	Deoxidation product
③	24.0	29.0	4.1	19.7	16.4	1.4	0.7	1.3	/	Ladle slag
④	75.4	19.4	/	1.0	2.0	2.3	/	/	/	Broken refractory

Fig.11 Typical inclusions extracted by Slimes from steel samples of the ladle (a), tundish (b) and slab (c)

Three kinds of inclusion size distributions are shown in **Figs.12-14**. Figure 12 is the inclusion number per unit 2-dimensinal section area by microscopic observation. Figure13 is the weight of large inclusions per 10 kg steel extracted by Slime method, which is similar to the inclusion mass fraction to steel. Both Fig.12 and Fig.13 have large histogram "bin" sizes. Inclusions extracted by Slimes test were suspended in water and their size distributions measured with a Coulter counter to get a 3-dimentional inclusion size distribution. This obtained the 3-dimensional size distribution up to 62μm. The curves were extrapolated to around 120μm as given in Fig.14 by matching to the measured amount of extracted inclusions larger than 50μm. The inclusions mass fraction is 66.8ppm in the tundish, 57.7ppm in the 20mm thickness nearest the slab surface, and averaging 51.9ppm in the slab. This suggests that inclusions in the interior of the slab (i.e., except outer 20mm thickness of the slab) is 50.6ppm. The fraction of inclusions removed from tundish to slab is around 22%.

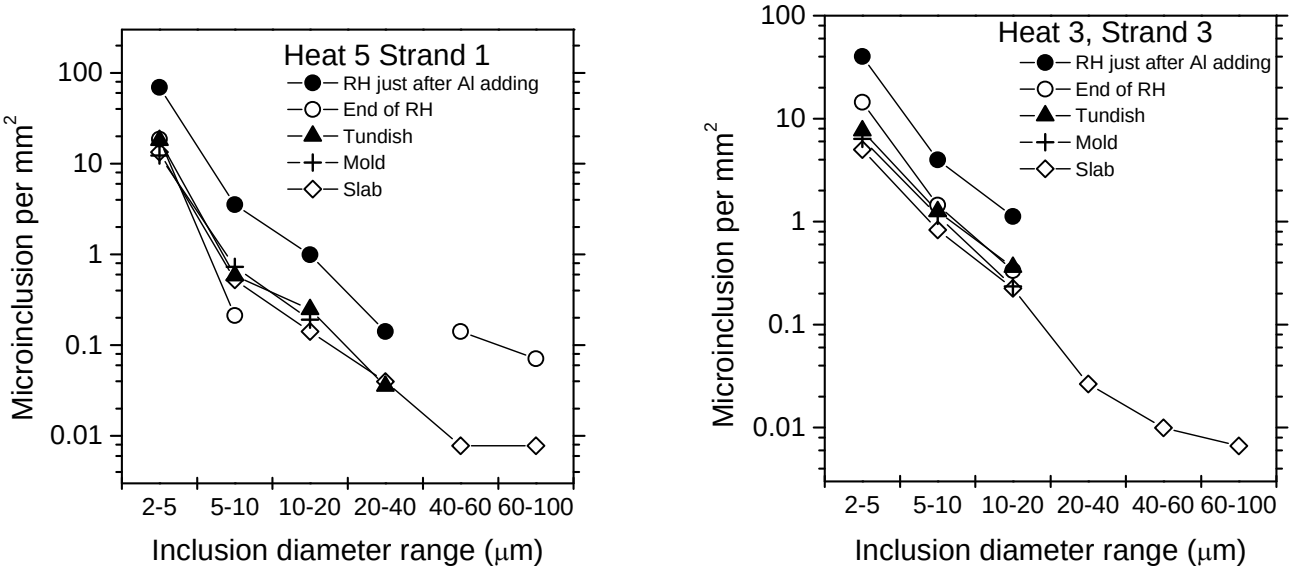

Fig.12 Microinclusion size distribution by the microscope observation

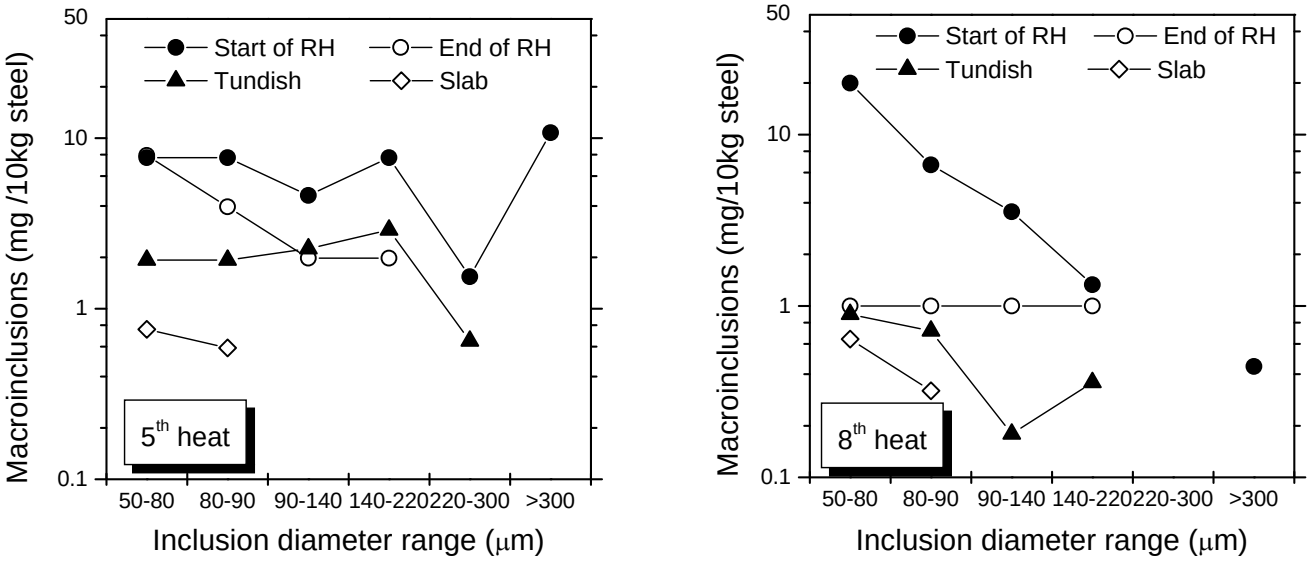

(a) (b)

Fig.13 The size distributions of large inclusions by Slime extraction

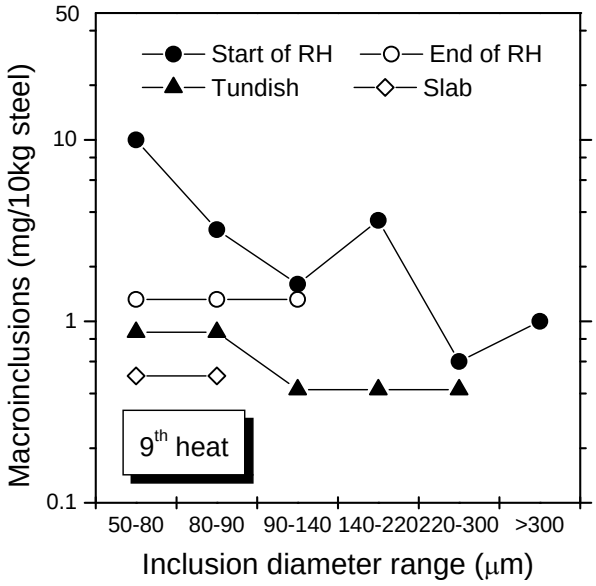

Fig.13 (c) The size distributions of large inclusions by Slime extraction

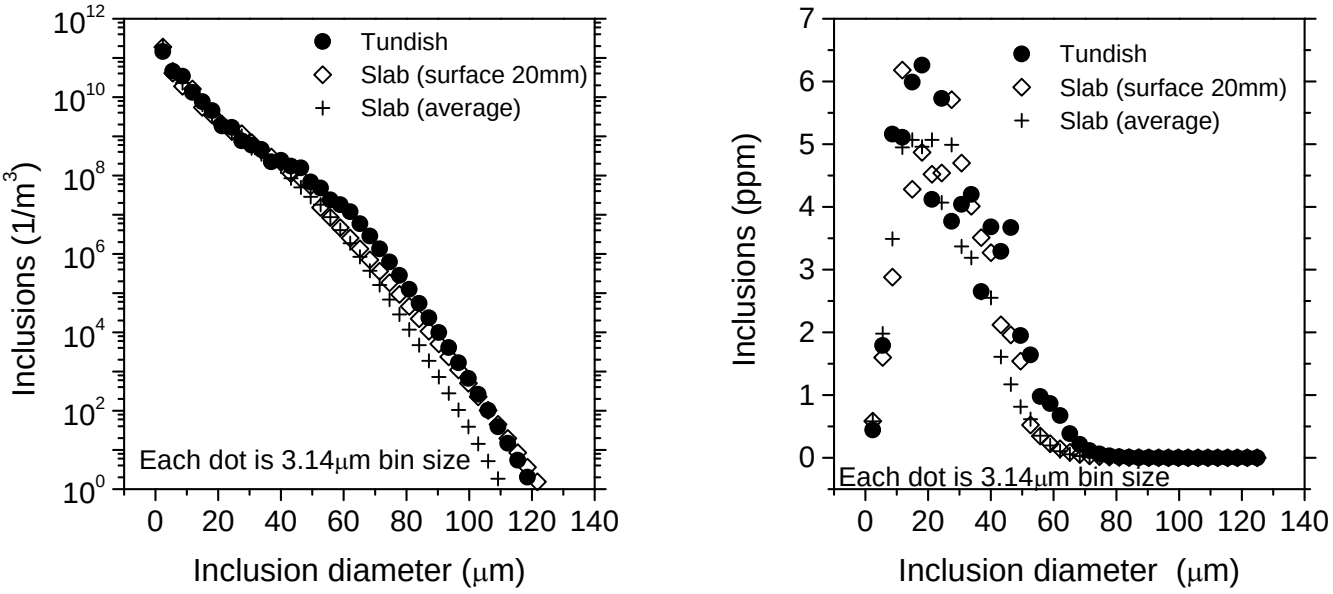

Fig,14 Inclusion size distribution evolution by Coulter Counter measurement of the Slime extracted inclusions

MATHEMATICAL SIMULATION OF FLUID FLOW AND INCLUSION BEHAVIOR

Steady flow in the Ar-stirred ladle, tundish and continuous caster were simulated with a 3-D finite-difference computational model using the standard k-ε turbulence model in Fluent [9]. Inclusion trajectories are calculated by integrating each local velocity, considering its drag and buoyancy forces. A "random walk" model is used to incorporate the effect of turbulent fluctuations on the particle motion. In this model, particle velocity fluctuations are based on a Gaussian-distributed random number, chosen according to the local turbulent kinetic energy. The random number is changed, thus producing a new instantaneous velocity fluctuation, with a frequency equal to the characteristic lifetime of the eddy.

Fluid Flow and Inclusion Behavior in Argon-Stirred Ladles

As previously discussed, inclusions can be removed during ladle steel refining especially during argon bubbling process. Thus, the flow and inclusion motion in an Ar-stirred ladle was simulated using an axisymmetric Lagrangian-Lagrangian multiphase model. Flow in the Baosteel 300 tonne ladle blown at 0.5 Nm^3/min using 900 32.7 diameter bubbles is shown in **Fig.15**. The bottom injected argon bubbles generate recirculation rolls, with a characteristic flow up the center and down the walls. **Figure 16** shows the calculated mixing time based on 99% mixing is 103-272s depending on 7 locations illustrated in **Fig.17**. This roughly matched experimental measurements [10]. The typical trajectories of 50μm, 100μm and 300μm inclusions are shown in Fig.17 and their residence time and trajectory length are shown in **Table VIII**, based on groups of 5000 particles. A typical 100μm inclusion moves 47.0m on its path through the ladle and is removed from the top surface after 285s. Actually, many inclusions enter the gas column shown in Fig.17. If they are captured by a bubble, they will be quickly removed because bubbles float out < 4s. Thus, bubble interactions greatly improve inclusion removal [11].

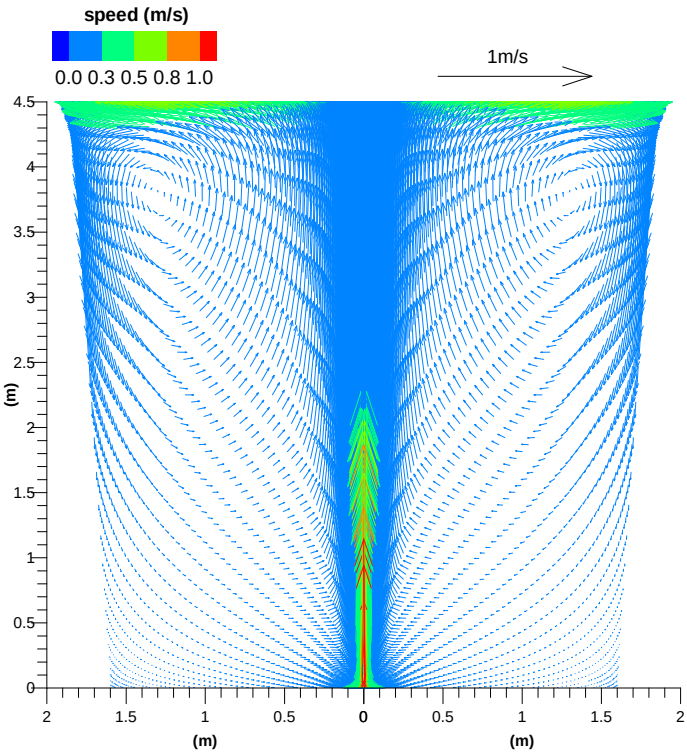

Fig. 15 Velocity vector distribution in argon-stirred ladle

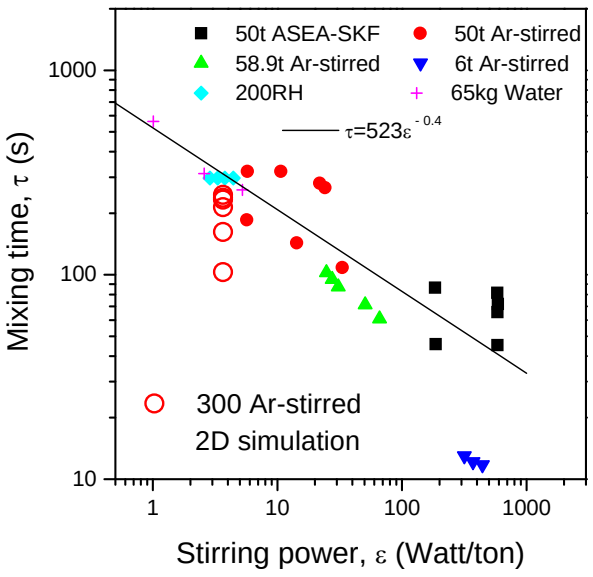

Fig.16 Mixing time *versus* stirring power

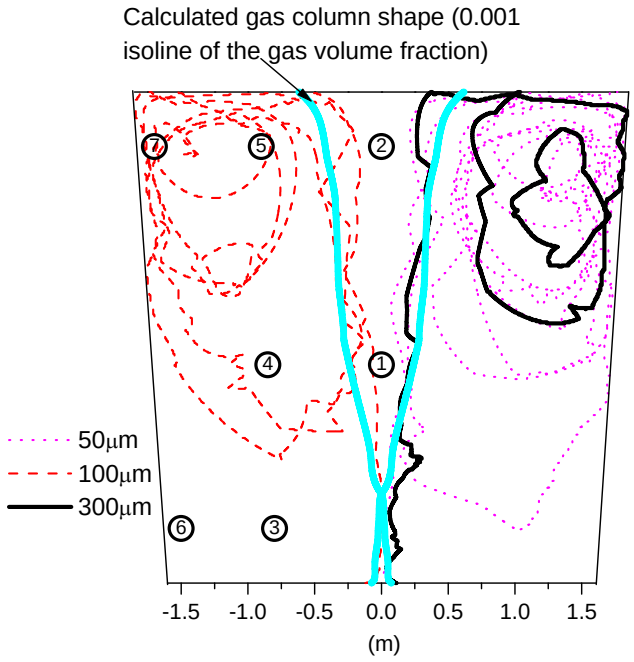

Fig.17 Typical inclusion trajectories and gas column shape

Table VIII Particle residence time and trajectory length in the Ar-stirred ladle

Particles	Argon bubble	Alumina inclusions		
Diameter	32.7 mm	50μm	100μm	300μm
Average path length (m)	5.0	58.0	47.0	24.0
Average residence time (s)	3.9s	327.8	284.9	147.1

Fluid Flow and Inclusion Behavior in Tundish

Fluid flow in three different 60 tonne tundish configurations are simulated in the current study: Tundish A—no flow control devices, Tundish B and C as indicated in Table I and Fig.1. The fluid flow patterns and characteristics are compared in **Fig.18** and **Table VIV**. In Table VIV, "Zone I" is the volume between the two weirs, and "Zone O" is the right of weir. The flow control devices restrain the vigorous turbulence in Zone I, where the stirring power is several hundred times higher than Zone O. The vigorous turbulence in Zone I favors the collision of inclusions, while the smoother flow pattern in Zone O favors inclusion removal to the top surface.

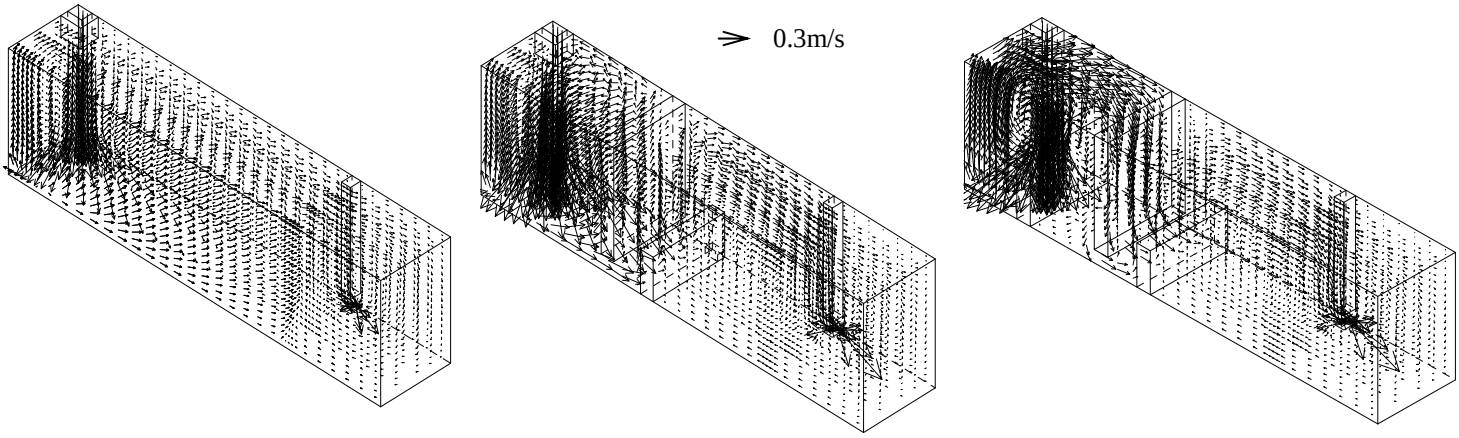

(a) Tundish A (b) Tundish B (c) Tundish C

Fig.18 Fluid flow patterns in tundish with different flow control devices

Table VIV Simulated flow characteristics of the tundish

Tundish	A(without flow control)		B(weir+dam)		C(weir with filter+ two dams)	
	Zone I	Zone O	Zone I	Zone O	Zone I	Zone O
$\overline{U}$ (m/s)	0.12	5.3×10^{-3}	0.13	7.1×10^{-3}	0.15	6.2×10^{-3}
Re	1.5×10^{5}	6.7×10^{3}	1.65×10^{5}	9.0×10^{3}	1.9×10^{5}	7.9×10^{3}
ε (m^2/s^3)	9.6×10^{-3}	9.3×10^{-5}	1.3×10^{-2}	3.1×10^{-6}	5.3×10^{-2}	1.6×10^{-6}

Inclusion growth by collision, removal by floating to the top surface and sticking to lining walls are modelled next. The collision model considers turbulent, Brownian and Stokes collision. [12] The removal of inclusions by sticking to the wall can be described as follows

$$\frac{\mathrm{d}n(r)}{\mathrm{d}t} = -M\, r^2\, n(r), \tag{5}$$

where M is expressed by

$$M = \frac{0.58\times10^{-2} u_\tau^3 r^2 \times10^{-12}}{\nu^2} A. \tag{6}$$

The shear velocity can be represented by

$$u_\tau = 0.173\overline{U}\,\mathrm{Re}^{-1/10}, \qquad (7)$$

where $\overline{U}$ and Re are volumetric based average velocity and Renolds number, given in **Table VIV.**
The calculated removal fraction of inclusions to different places is shown in **Table X**. In this table, the removal fraction is in percentage from ladle to tundish according to Eq.(1). Without flow control (tundish A), around 36.2% inclusions are removed to the top surface, and 14.8% stick to the walls. With flow control devices, floating to the top slag increases to 43-50%, and sticking to walls to 21-30%. This agrees with some of the measurements in **Table V**, especially the measurement of macroinclusions.

Table X Inclusion removal fractions to different tundish places

Tundish		A	B	C
Floating to top surface		**36.2**	**43.1**	**49.5**
Sticking to lining	Long wall	10.2	11.1	12.3
	Side wall	1.3	0.8	0.9
	Bottom	3.3	4.1	6.2
	First dam	/	/	1.5
	Weir	/	3.7	/
	Weir+filter	/	/	7.2
	Second dam	/	1.3	1.4
	Total	**14.8**	**21.0**	**29.5**
Total (%)		**51.0**	**64.1**	**79.0**

Fluid Flow and Inclusion Behavior in Continuous Caster

The fluid flow pattern inside the SEN and the computed locations of inclusions that attach to the SEN walls are shown in **Fig.19**. The calculation suggests that around 12% of the inclusions leaving the tundish stick to the SEN walls (removed by clogging). Figure 19 suggests uniform buildup on the nozzle walls, with increased tendency towards buildup on the SEN bottom due to impact from the flowing jet. This is consistent with observations of nozzle clogging where local reoxidation or chemical interaction were not the cause.

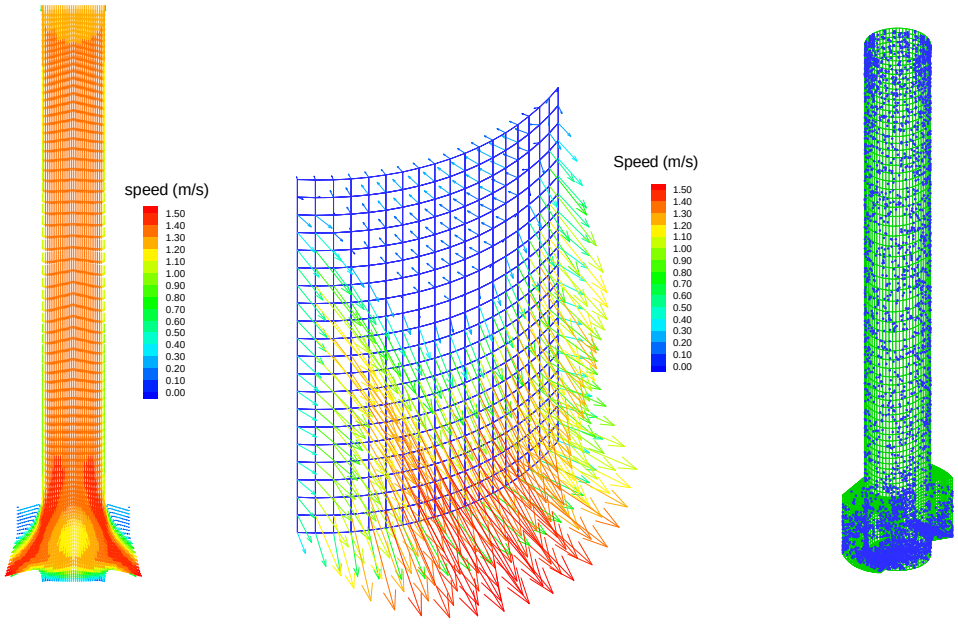

Fig, 19 Fluid flow pattern in the SEN and inclusion locations sticking to SEN walls

The corresponding fluid flow pattern in the centerline section through the wide face of the 3-D half-mold simulation and the positions of entrapped 50 μm inclusions on the solidified shell are shown in **Fig. 20**. **Table XI** compares inclusion fractions entrapped at different destinations with the industrial measurement. For inclusions smaller than 50 μm entering the mold, only 7% are safely removed by the top surface (6% from tundish to slab in Table XI), independent of inclusion size. A larger fraction of inclusions bigger than 50 μm are removed. The majority of inclusions leaving the tundish (57%) are captured within 28mm of the surface, which represents the top 2.55m of the caster. This agrees only qualitatively with measurements in Fig. 7. A disproportionately large fraction of these (21%) are captured in the narrow face, despite its smaller surface area, owing to the jet impingement against its inner solidification front. Inclusions exiting the domain are entrapped somewhere deeper than 28mm. If the entrapment criteria are the same for small and large inclusions, their entrapment to walls is very similar at 0-28mm slab surface thickness. Only 7-12% of the inclusions entering the mold are predicted to be removed by the top surface (6-11% from tundish to slab in Table XI). Adding 12% sticking to SEN walls, the simulated inclusion removal from tundish to slab is 18-23%, which aggress well with the measurement of 22% calculated from Fig. 14.

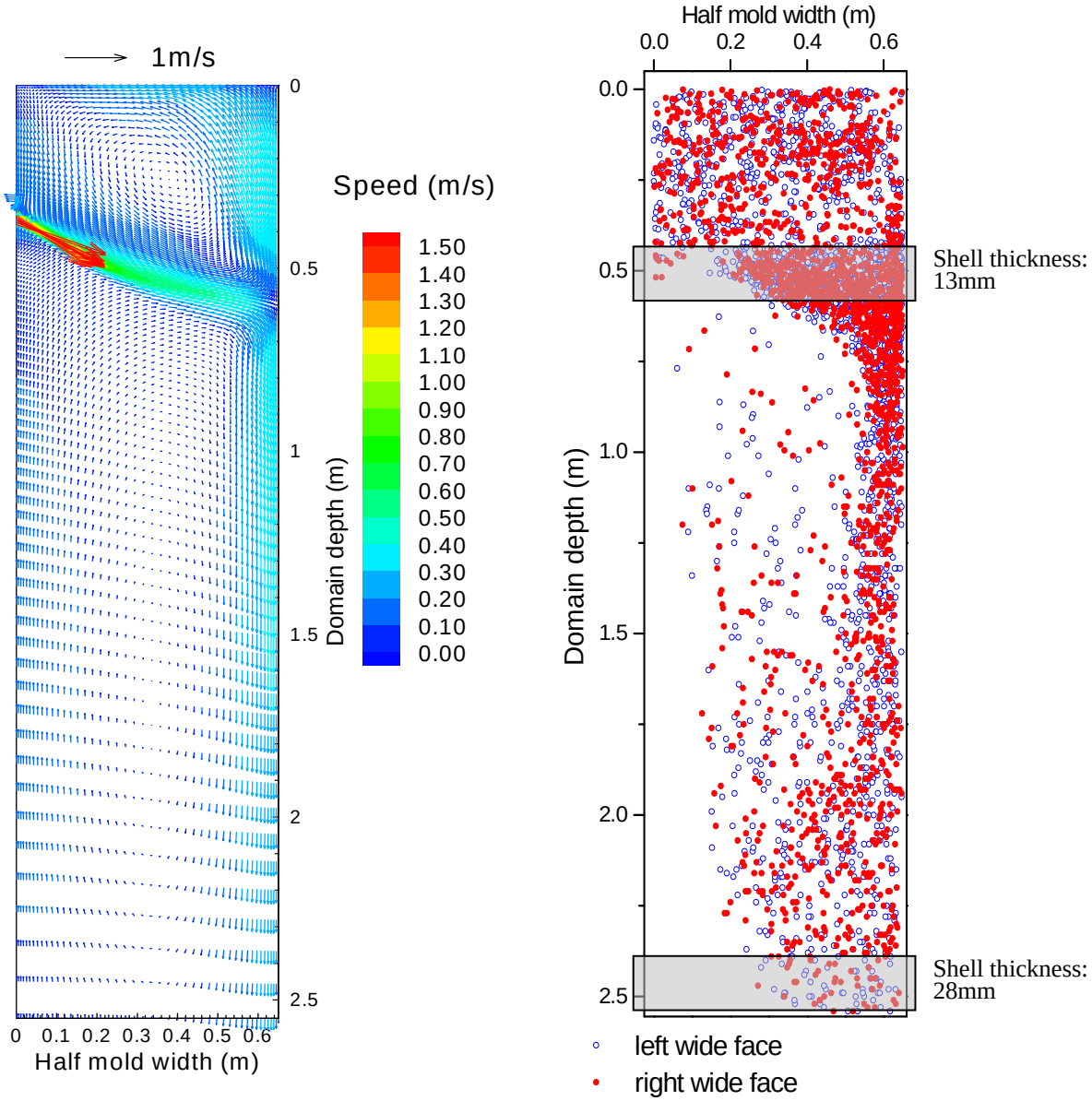

Fig.20 Fluid flow pattern on the central half wide face and 50 μm inclusion entrapped positions on the solidified shell of half wide face

Table XI. Fractions of inclusions entrapped at different locations after leaving tundish

Simulation	Size	SEN walls	Top slag of mold	Slab				
				Narrow face		Wide face		Interior
				0-15mm	15-28mm	0-15mm	15-28mm	28-125mm
	50μm	**12%**	**6%**	11%	9%	24%	13%	25%
	225μm	**12%**	**11%**	12%	9%	26%	10%	20%
Measurement	All	**22%** (decrease from tundish to slab)						

SUMMARY

1. Plant measurements of many samples have systematically evaluated steel cleanliness at every processing step at Baosteel.

2. Through clean-steel practice, [C]+T.O.+[N]+[P]+[S] in the slab can be simultaneously controlled to ~100ppm consisting of 10-20ppm total oxygen, 10-30ppm nitrogen, 20-40ppm sulfur, 20ppm phosphorus, 30ppm carbon.

3. Reoxidation balances on the ladle during RH treatment and the tundish found that reoxidation accounts for about 20% of the total oxygen in RH treatment, and about 50% in the tundish

4. The typical morphologies of inclusions are angular aluminate, alumina cluster, and spherical silicate. The possible sources are deoxidation products, reoxidation product, slag entrapment or broken refractory lining bricks.

5. Inclusions concentrate most within 20mm of the slab surface. Some slabs have occasional concentration at the ¼ slab thickness from the inner radius, mainly induced by the entrapment of released clogged materials from the SEN during ladle exchanges.

6. Steady flow and inclusion trajectories in an Ar-stirred ladle, tundish and continuous caster are simulated with the standard k-ε turbulence model. In Ar-stirred ladles, inclusions may circulate a long distance, but those captured in the gas column quickly float to the top slag. In the tundish, flow control devices constrain the vigorous turbulence to the inlet zone, which remove inclusions 13-28% higher than without flow control devices

7. In the continuous caster, around 12% of inclusions leaving the tundish are removed by sticking to the SEN walls, and only 6-11% are predicted to be removed to the top slag of the mold. This roughly matches the measured total inclusion removal fraction to the top surface of 22%. The majority of simulated inclusions entering the mold (65%) are captured within 28mm of the surface of the slab, which represents the top 2.55m of the caster.

ACKNOWLEDGEMENTS

The authors are grateful for support from the National Science Foundation (Grant No. DMI-0115486), the Continuous Casting Consortium and the National Center for Supercomputing Applications at the University of Illinois. The authors also wish to thank Baosteel, University of Science and Technology Beijing, and the Central Iron and Steel Institute (P.R.China) for sampling and analysis.

REFERENCES

1. K.W. Lange, "Thermodynamic and Kinetic Aspects of Secondary Steelmaking Processes," Inter. Materials Reviews, Vol. 33 (2), 1988, 53-89.
2. W.B. Morrison, "Nitrogen in the Steel Product," Ironmaking & Steelmakaing, Vol. 16 (2), 1989, 123-130.
3. L. Zhang and B.G. Thomas, "State of the Art in Evaluation and Control of Steel Cleanliness," ISIJ Inter., 2003, in press.
4. A.W. Cramb, "High Purity, Low Residual and Clean Steels," in Impurities in Engineered Materials: Impact, Reliability and Control, J.W. C. L. Briant, ed., 1999, 49-89.
5. R. Kiessling, "Clean Steel- a debatable concept," Met. Sci., Vol. 15 (5), 1980, 161-172.
6. N.A. McPherson and A. McLean, Continuous Casting Volume Seven - Tundish to Mold Transfer Operations, Vol. 7, ISS, Warrendale, PA, 1992, 1-61.
7. D. Mu and L. Holappa, "Production of Clean Steel: Literature Survey," Report No. PB93-179471/XAB, Gov. Res. Announc. Index (USA),, 1993.
8. L. Zhang, X. Jing, L. Zhu, K. Cai, "Mathematical Model of Decarburization of Ultra Low Carbon Steel during RH Treatment," Journal of University of Science and Technology Beijing(English Edition), Vol. 4 (4), 1997, 19-23.
9. FLUENT5.1, Report, Fluent Inc., Lebanon, New Hampshire, 2000.
10. T.C. Hsiao, T. Lehner and B. Kjellberg, "Fluid Flow in Ladles-Experimental Results," Scand. J. Metallurgy, Vol. 8, *1*980, 105.
11. L. Zhang and S. Taniguchi, "Fundamentals of Inclusion Removal from Liquid Steel by Attachments to Rising Bubbles," I & Smaker, Vol. 28 (9), *2*001, 55-79.
12. L. Zhang and S. Taniguchi, "Fluid Flow and Inclusion Removal in Continuous Casting Tundish," Metal. & Material Trans. B., Vol. 31B (2), *2*000, 253-266.